J Math Chem (2014) 52:1414–1440
DOI 10.1007/s10910-014-0320-6

ORIGINAL PAPER

Microvia fill process model and control

Antti Pohjoranta · Robert Tenno

Received: 11 November 2013 / Accepted: 27 January 2014 / Published online: 8 February 2014

Abstract This paper presents an overview of the modeling and model based control of the microvia fill process. A detailed, general-purpose microvia fill model that utilizes the arbitrary Lagrange–Eulerian method for shape change modeling is presented first. Modeling results are presented and compared with the measured data. Then a simplified model of the process is presented followed by a model based control algorithm being developed based on the simplified stochastic model with typical uncertainties induced by unmodelled phenomena and measurement error. The developed control algorithm is analyzed in terms of possible control errors and applied to control the firstly presented microvia fill process model.

Keywords Microvia filling · Microvia fill control · Microvia fill modeling · Deposition control

1 Introduction

Multilayered printed circuit boards (MLBs or PCBs) are nowadays basic building elements of microelectronic devices. With the circuitry running in even 50 or more layers, they enable packing the electronic components of the device within a significantly smaller footprint than if only a single layer PCB was used. Microvia filling, a process in which the interconnections between adjacent circuit layers are formed, is a key step in the series of sub-processes required in the entire manufacturing process for

A. Pohjoranta (✉)
Fuel Cells, VTT Technical Research Centre of Finland, Espoo, Finland
e-mail: antti.pohjoranta@vtt.fi

R. Tenno
School of Electrical Engineering, Aalto University, Espoo, Finland
e-mail: robert.tenno@aalto.fi

MLBs. The process takes place in an electrolytic copper plating bath, where the copper reduction rate at different sites of the board is significantly affected by surfactant chemicals added in the bath. It is of primary interest to the process operator to both understand and to be able to administrate the process as well as possible. Changes in the process operating parameters need to be done if the product parameters (such as via size and shape) change and as the process bath ages. A process model is an excellent tool for quickly and cheaply studying the process behavior under a variety of operating conditions, without actually needing to execute time-consuming and costly experiments in a research site, or worse still, at the production line. A process model also enables the development of automatic control of the process, which can help to run the process more accurately in the way the operator intends to.

This paper discusses the computational modeling of the microvia fill process, from both a process modeling aspect as well as in the framework of automatic process control. For these purposes, a highly detailed distributed parameters model of the microvia fill process is presented first, followed by a less complex, control-oriented model and a discussion of its application for process control. The experimental parts related to this work are found in the cited references and their detailed discussion is omitted from this paper. The paper summarizes previous work on the process modeling [23] and control [24,25,28,29]. Finally, as new a contribution, the control developments are applied to control the modeled via fill process.

Although the model is developed for the microvia fill process, utilized in PCB manufacturing, the model surface chemistry is similar to the damascene process surface chemistry with of 2–3 additive components (suppressor, accelerator and possibly leveller additive) in a $CuSO_4$ bath with sulphuric acid as supporting electrolyte. The suppressor and accelerator additive names refer to additive complexes with adsorbed chloride.

Significant research efforts related to the copper electroplating process with additives has been carried out by several groups. Although numerous other and significant contributions to the topic have been brought, the work of Moffat et al., e.g. [1–5], Dow et al., e.g. [6–8], Andricacos et al. [9,10], West et al., e.g. [11–13] should be mentioned in particular as they have strongly influenced the work behind this paper.

2 The microvia fill process model

The microvia fill process is a complex electrochemical process where surfactants acting on the plated copper surface play a significant role [14,15]. The surfactant and copper interaction chemistry has been extensively studied by several groups in terms of both PCB production as well as integrated chip manufacturing as copper electroplating is utilized there also [1–3,6–10]. Evidently, the system of equations utilized for the computational modeling of microvia filling should describe the processes occurring in both the non-bulk electrolyte (which is the main modeling domain) as well as on the copper surface (which is a domain boundary). The circular shape of the microvia enables simplifying its model geometry as the model equations can be formulated only in two spatial dimensions (2D) by utilizing the axial symmetry of the modeled domain. As the modeling domain shape change is characteristic to the microvia fill process, its effects have to be included in the solution somehow. In this work series,

the arbitrary Lagrange–Eulerian (ALE) method, e.g. [16], is utilized to capture the domain shape change.

The equations used in a basic microvia fill process model are discussed next. For brevity, the explanation of most equation symbols is omitted from the text and the symbols along with their explanations are compiled in Table 1.

The basis of copper electrolysis is given by the Cu/Cu^{2+} system electrochemical reaction Eq. (1).

$$Cu^{2+}\,(aq) + 2e^- \rightleftarrows Cu(s), \quad \Delta\phi^0_{eq} = +0.34\,V \tag{1}$$

If neglecting side-reactions and current efficiency, the rate of reaction (1) can be considered directly proportional to the current density i_e (A/m^2) on the electrode surface where the reaction takes place. As every electrochemical system, also the microvia filling bath has two electrodes—the anode and the cathode, whereby $e = a, c$, respectively—and the electrochemical equations apply to both electrodes in the bath. Furthermore, typically both electrodes in a microvia filling bath are made of metallic copper, significantly simplifying the treatment.

The current density i_e is given by the Butler–Volmer equation (2), which is a non-linear equation relating the electrode overpotential η_e (V) and the copper ion activity at the electrode $a_{e,}$ with the said current density.

$$i_e = i_{0,e}\left(a_{a,e}\mu_{a,e}e^{k\alpha_{a,e}\eta_e} - a_{c,e}\mu_{c,e}e^{-k\alpha_{c,e}\eta_e}\right) \tag{2}$$

In (2), the second subscript is for the forward (cathodic) and backward (anodic) reactions. The multiplier $\mu_{e,}$ is utilized to implement the effects that surfactant chemicals that are active on the surface of electrode e have on the rate of the copper redox reaction (1).

Typically only $\mu_{c,c}$, i.e. the term affecting the cathodic reaction (reduction) on the cathode is essential and $\mu_{a,i}$ and $\mu_{c,a}$ are considered equal to 1.

The electrode overpotential is defined as difference of the electrode potential $\Delta\phi_e$ from the equilibrium potential $\Delta\phi_{eq,e}$ as in (3).

$$\eta_e = \Delta\phi_e - \Delta\phi_{eq,e} \tag{3}$$

The equilibrium potential for the electrode is obtained based on the standard equilibrium potential and the thermodynamic state of the electrode as given in (4).

$$\Delta\phi_{eq,e} = \Delta\phi^0_{eq,e} + k^{-1}\ln(a_e) \tag{4}$$

The current densities of the electrodes are coupled by the total current, which at both electrodes must be equal (but opposite signed).

$$A_a i_a + A_c i_c = 0 \tag{5}$$

Similarly, the electric circuit formed by the filling bath system must abide to Kirchoff's laws, especially, so that the voltage steps when going over the whole circuit sum up to zero.

Table 1 List of symbols and coefficients

Symbol	Description	Unit
A_e	Area of electrode e	m^2
a_i	Activity of species i	–
α_i	Apparent transfer coefficient of process i	–
A, B	Linear operators	–
c	The Cu^{2+} ion concentration	mol/m^3
c_i	Concentration of species i	mol/m^3
c^0_{Cu}	Reference concentration of the Cu^{2+} ion, 1,000	mol/m^3
c^{lim}	A limit concentration of species, 3.5 (empirical)	mol/m^3
D	Diffusion coefficient of the Cu^{2+} ion	m^2/s
D_i	Diffusion coefficient of species i	m^2/s
$D_{s,i}$	Surface diffusion coefficient of species i	m^2/s
δ	Thickness of the electrolyte layer with diffusion dominated mass transfer	m
E_{OUT}	Output voltage of an electrolysis cell power source	V
e^κ	Function set	–
η_e	Overpotential at an electrode e	V
F	Faraday's constant, 96,485	As/mol
$\mathbf{F}$	Deformation gradient (matrix)	–
ϕ	Electric potential	V
$\Delta\phi_e$	Electrode potential versus the standard hydrogen electrode	V
$\Delta\phi_{e,eq}$	Equilibrium potential of the Cu^{2+} ion redox reaction at electrode e	V
$\Delta\phi^0_{eq}$	The standard potential of the Cu^{2+} ion redox reaction, 0.34	V
$\Gamma_i, \quad \Gamma_i^{max}$	Surface concentration of species i and its maximum value	mol/m^2
γ	Noise spatial correlation power	–
i_e	Current density at electrode e	A/m^2
$i_{e,0}$	Exchange current density of the reaction at electrode e	A/m^2
j	Discrete location point index, $j = 1, 2, 3 \ldots N$	–
k	Shorthand for $z_{Cu}F/R/T$, 77.85	1/V
k_i^p	Adsorption, desorption or consumption of additives i	m^3/mol/s, 1/s, m/s
K_P	Control gain	m/s
κ	Identifier: noise type, $\kappa = 0, d, \delta$	–
$m, \mathbf{M}$	Expected value (of $c(t)$) and the expectation operator	–
μ	Coefficient for surfactant effects on the copper redox reaction	–
N_i^p	Surface mass transfer flux of species i due to process p	$mol/m^2/s$
n_i	Rate of reaction i and the associated mass flux	$mol/m^2/s$
$\mathbf{n}$	Model boundary outward normal vector	–
R	Ideal gas coefficient, 8.314	J/mol/K
ρ_i	Density of species i	kg/m^3
ρ^κ	Noise intensity term in domain κ	mol/m^3

Table 1 continued

Symbol	Description	Unit
s^{κ}	Noise focus term in domain κ	m
σ	Conductivity of the electrolyte	S/m
σ_j^{κ}	Intensity of noise of type κ at site j	–
T	Temperature	K
t	Time	s
θ_i	Surfactant surface coverage of species i	–
U_{Ω}	Voltage drop due to ohmic resistance of the electrolyte	V
u	The control variable (exercised through boundary)	mol/m^2/s
$\mathbf{v}$	Mesh movement velocity (vector)	m/s
x	Location (distance from cathode)	m
W_j^{κ}	Standard Wiener process in domain κ at site j	–
$\mathbf{x}$, $\mathbf{X}$	Location at deformed and reference coordinate systems	m
z_i	Electron number of species i	–
∇_{T}	Surface tangential differential operator	–

$$E_{OUT} + \eta_a - \eta_c + U_{\Omega} = 0 \tag{6}$$

For the practical application of (2) and (4), means to approximate the copper ion activity are required and in this paper the concentration based formula (7) is utilized. This formula is obtained based on measurements against a Cu/Cu^{2+} reference electrode as described in [17].

$$a_{c,e} \approx \frac{c_{\mathrm{Cu},e}}{c^0_{\mathrm{Cu}}} \left(\frac{c_{\mathrm{Cu},e} + c^{lim}}{c^0_{\mathrm{Cu}} + c^{lim}} \right)^{-0.56} \tag{7}$$

The mass transfer of species i within the main modeling domain, i.e. the electrolyte solution is described by (8). The considered species include the main ions (Cu^{2+}, H$^+$, SO$_4^{2-}$, HSO$_4^-$) as well as the additive species, which are considered not charged. For the non-charged species, (8) reduces to the diffusion equation. It is considered that due to the continuous agitation of the microvia fill bath electrolyte, species' concentration in the bulk of the bath have a constant bulk concentration and only the mass transfer within a thin layer of electrolyte close to the electrode surface, where diffusion and migration dominate mass transfer, has to be modeled explicitly.

$$\frac{\partial c_i}{\partial t} = \nabla \cdot (D_i \nabla c_i) + \nabla \cdot \left(z_i F \frac{D_i}{RT} c_i \nabla \phi \right) \tag{8}$$

Mass transfer of electrically charged species (Cu^{2+}, H$^+$, SO$_4^{2-}$, HSO$_4^-$) is also restricted by the electroneutrality condition (9). However, it is also completely possible to exclude this equation from the computational system and still obtain functioning models. (It may be considered that because the H$^+$ has such a high diffusivity compared

to the other ions as well as a very high concentration, the electroneutrality condition is well enough satisfied by the very mobile H^+ ions even without the condition.)

$$\sum z_i c_i = 0 \tag{9}$$

As there is current flowing through the electrolyte and ionic species are involved, following the conservation of electric charge principle (10) should be taken care of.

$$\nabla \cdot \mathbf{i} = 0 \tag{10}$$

The current density $\mathbf{i}$ in (10) is the ionic current density in the electrolyte that satisfies (11).

$$\mathbf{i} = F \sum z_i \left(D_i \nabla c_i + z_i F \frac{D_i}{RT} c_i \nabla \phi \right) \tag{11}$$

The electric potential field ϕ abides to the Laplace equation (12), where the electrolyte conductivity can be approximated by various means, for example (13).

$$\nabla \cdot (\sigma \nabla \phi) = 0 \tag{12}$$

$$\sigma = \frac{F}{RT} \sum z_i^2 D_i c_i \tag{13}$$

Since a supporting electrolyte is typically used in the via fill electroplating bath, the mass transfer the metal ions by migration can be considered insignificant related to diffusion. This enables simplifying the computational model.

Equations (1) to (13) summarize the basic electrochemical and thermodynamic phenomena of the microvia fill process that take place in the non-bulk electrolyte domain. Since they are formulated as PDEs, also suitable boundary conditions should be given.

The mass flux and current density over any boundary are coupled by (14).

$$i_e = \sum n_{a,i} F z_i \tag{14}$$

The mass flux over an electrode boundary is given by (15), where $\mathbf{n}$ is the boundary outward normal vector.

$$\mathbf{n} \cdot \left(D_i \nabla c_i + z_i F \frac{D_i}{RT} c_i \nabla \phi \right) = n_{a,i} \tag{15}$$

Similarly, the ionic electrode current density is given by (16), and the actual boundary conditions for the electric and mass transfer systems are obtained by coupling Eqs. (14) and (15).

$$\mathbf{n} \cdot F \sum z_i \left(D_i \nabla c_i + z_i F \frac{D_i}{RT} c_i \nabla \phi \right) = i_e \tag{16}$$

The boundary condition for the electrically neutral additives is taken simples as the 1st order reaction at this boundary

$$\mathbf{n} \cdot (D_i \nabla c_i) = N_i^{cons}$$

The surfactants' effect is brought to the model through the surfactants' surface concentration on the active copper electrode surface. Several surfactants, such as suppressors, accelerators or leveler may be considered and their mass transfer processes, taking copper electrode surface can be summarized into the generically formulated Eq. (17).

$$\frac{\partial \Gamma_i}{\partial t} = -\Gamma_i \left(\nabla_{\mathrm{T}} \cdot \mathbf{v}_T\right) - \Gamma_i \left(\nabla_{\mathrm{T}} \cdot \mathbf{n}\right)(\mathbf{v} \cdot \mathbf{n}) + D_{s,i} \nabla_{\mathrm{T}}^2 \Gamma_i + N_i^{ads} - N_i^{des} + N_i^{cons} \tag{17}$$

Equation (17) accounts for changes in surfactant's i (i = suppressor, accelerator, leveler) surface concentration Γ_i due to the following surface phenomena (from left to right, on the right-hand side of (17)):

(i) surface deformation in the surface tangential direction (i.e. for surface stretching and compression)
(ii) surface deformation due to the movement of a curved surface in its normal direction
(iii) diffusion of the surfactant along the surface due to a surface concentration gradient
(iv) other processes (p = *ads, des, cons*) such as chemical decomposition, absorption into the metal as well as adsorption and desorption, collected in the source terms N_i^p, whose sign should be set appropriately (negative for consuming process, positive for producing process)

The boundary conditions for (17) are in practice point conditions (in a 2D model) and a symmetry condition was used in this work.

The additives' behavior on the copper surface has been under significant research. Several formulations for the adsorption and desorption as well as consumption processes are given in the literature [2,6,9,12,18]. The best describing formulation of course depends on the chemical system in question. In this work, Eqs. (18) and (19) are used for the adsorption (*ads*) and desorption (*des*) for the suppressor (*supp*) and accelerator (*acc*), leveler (*lev*) additives, and equations of the form (20) for the consumption (*cons*) of the additives.

$$N_{supp}^{ads} - N_{supp}^{des} = k_{supp}^{ads} c_{supp} \left(\Gamma_{supp}^{max} - \Gamma_{supp} - \frac{\Gamma_{supp}^{max}}{\Gamma_{acc}^{max}} \Gamma_{acc}\right) - k_{supp}^{des} \Gamma_{supp} \tag{18}$$

$$N_i^{ads} - N_i^{des} = k_i^{ads} c_i \left(\Gamma_i^{max} - \Gamma_i\right) - k_i^{des} \Gamma_i \tag{19}$$

$$N_i^{cons} = k_i^{cons} c_i \tag{20}$$

In the computational implementation, the surface concentration is often scaled with its maximum value to yield a dimensionless surface coverage $\theta_i = \Gamma_i / \Gamma_i^{max}$, whose

value ranges from 0 to 1 and is thus more suitable for computation and is easier to interpret.

Finally, the coupling of the copper reduction reaction rate and the surfactant coverage is made through the $\mu_{c,c}$ coefficient in (2). The simplest formulation for $\mu_{c,c}$, used e.g. in [23] is $\mu_{c,c} = 1 - \theta_{supp}$, where the suppressor additive species is some additive which has a blocking effect on the copper reduction reaction. The value which θ_{supp} obtains is determined through (17) and the interactions of all included surfactant species, implemented through N_i^p. In case of three additives in the system, the independent coverage $\mu_{c,c} = \left(1 - \theta_{supp}\right)(1 - \theta_{lev})$ is used in the model.

2.1 The electrode surface movement and ALE

In electrodeposition, the cathode surface moves as metallic copper is deposited. The surfactants' effect on the deposition rate in a via filling process has been shown to be closely related to the electrode surface curvature [2]. The electrode surface movement must be included in the via fill process by a means that effectively alters the geometry of the modeled domain during the computation. In this work, the ALE method was chosen for this purpose. Any other suitable method can be used, however, and also at least the level set, finite-volume and Monte Carlo methods have been utilized [5,19–21]. The ALE method can nowadays be found as a built-in tool in advanced PDE system solvers, such as the COMSOL Multiphysics software, which was used also by the authors.

The ALE method is a node tracking method, where the shape of the modeling domain is tracked explicitly. Tracking of the deforming domain is based on creating a mapping between the deformed and a reference (fixed) coordinate system. The mapping is obtained as the deformation gradient $\mathbf{F} = \partial\mathbf{x}/\partial\mathbf{X}$, where $\mathbf{x}$ and $\mathbf{X}$ are the location in the deformed and the reference coordinate systems, respectively. To carry out calculations of phenomena that occur in the deformed domain, their describing equations are transformed back to the reference system by using the inverse $\mathbf{F}^{-1}$.

The node points of the deformed mesh ($\mathbf{x}$) are obtained by integrating the mesh velocity $\mathbf{v}$ in time, with the initial condition $\mathbf{x} = \mathbf{X}$. The mesh velocity $\mathbf{v}$ is obtained by a mesh smoothing method and Laplacian smoothing was used by the authors due to its simplicity. (Also e.g. Winslow smoothing can be used.) This means that the mesh velocity is obtained by solving the Laplace equation $\nabla^2\mathbf{v} = 0$ for $\mathbf{v}$ as part of the equation system. The determinant $\det(\mathbf{F})$ yields the scaling factor between the two coordinate systems, which scales the infinitesimal integration element during solution the electrochemical system (2)–(20).

The coupling between the ALE solution and the electrochemical part is formed by the electrode boundary velocity, which is given as boundary condition to the ALE system. The electrode boundary moves due to the growth of the deposited copper layer and the movement velocity in the boundary normal direction is given by (21).

$$\mathbf{v} \cdot \mathbf{n} = i_c \frac{M_{\mathrm{Cu}}}{z_{\mathrm{Cu}} F \rho_{\mathrm{Cu}}} \tag{21}$$

The main weakness of the ALE method is in its intolerance to large deformations of the modeling domain—it does not allow for topology changes (which would occur e.g. when simulating the forming of a "hollow"/void via) without re-meshing of the domain. Indeed, computational accuracy is often lost as the mesh deforms dramatically, unless mesh improvement is carried out regularly. The main strengths of ALE are its simplicity and the relatively modest computational effort required to run it accurately.

A detailed description and analysis of implementing the surfactant mass balance computation in a moving geometry modeled by the ALE method is given by the authors in [22] and therefore further details of the geometry shape change formulation are omitted from this text.

2.2 Computational model

The discussed model is applied partly in computation and not all parameters of the model are specified. The Butler–Volmer equation (2) is specified for the cathode only. The surface overpotential is calculated from this equation and the Eqs. (3)–(6) related to the anode no need to specify. The opposite boundary to the cathode is the bulk solution boundary where the bulk concentration specifies the Dirichlet data there. The bulk solution boundary is the moving boundary with the same velocity as flat cathode surface. The zero flux (symmetry) conditions are used on other boundaries.

If the electroneutrality condition (9) is ignored, the number of species in (8) reduces. Only the Cu^{2+} ion and the additives, *Supp, Acc* need to be considered. Equations (14) and (15) are auxiliary and they explain Eq. (16) in equivalent form. In a simpler computational model the migration of ions in the electric field in (8) can be ignored and then the system (10)–(13) that solves the electric potential and expresses the current density in electrolyte is uncoupled from the rest of the system and therefore all the related parameters like output voltage E_{OUT} and ohmic resistance U_Ω of the electrolyte that depends on the current density and conductivity of the electrolyte that again depends on the concentration of all charged species (Cu^{2+}, H^+, SO_4^{2-}, HSO_4^-) do not need to be specified. From other side if such specification is made implementation of the ion migration in the electrochemical system is a relatively simple light extension computationally.

In the computational implementation, the surface coverage is calculated instead of surface concentration to simplify the parameterization. Furthermore, the chloride species, required in the additive complexes, is assumed to be sufficiently well provided on the cathode surface so that it does not limit the additives' effect and therefore does not need to be modeled explicitly.

2.3 Modeling results and discussion

The performance of the reported microvia fill process model is illustrated below. The model parameters used in the simulation are found in [23]. In Fig. 1, the simulated evolution of the copper deposit thickness at the via center and on the flat board surface versus time are compared to the measured values. The corresponding cross-sectional images of the via are shown in Fig. 2. In the reported case, a constant current was

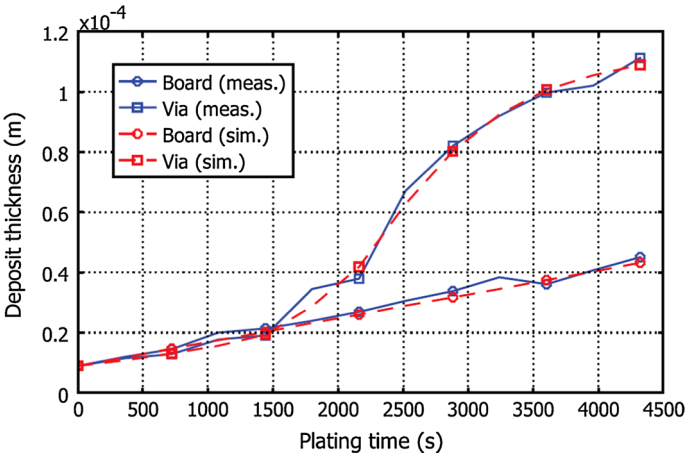

Fig. 1 The copper deposit thickness inside the via (*square*) and on the flat board surface (*circle*) plotted versus time. The simulated estimate is shown by the *dashed line* and the measured data with a *solid line*

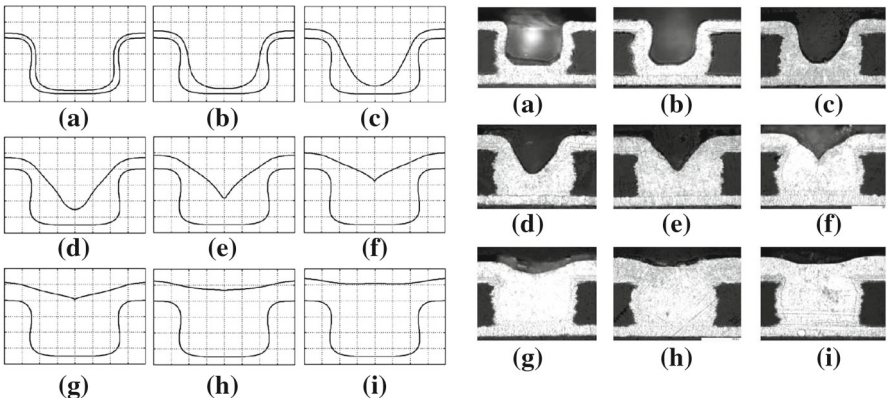

Fig. 2 Cross-section images of simulated (*left*) and measured (*right*) deposit evolution at different time instants into the via fill process. The time instants are **a** 12, **b** 18, **c** 24, **d** 30, **e** 36, **f** 42, **g** 48, **h** 54 and **i** 60 min. The data corresponds to that in [17]

applied over the electroplating cell. Simulation results with a controlled, time-varying current are given in Sect. 3.

Although the model reported here was tested against practical data [17,23] obtaining measurement data of via growth during the fill process is laborious and so the test cases were only few. Therefore, at least before further validation, it should be considered that the model is primarily a qualitative tool for examining the effects of various changes in the process conditions. Furthermore, even if an accurate parameterization of the model was reliably found, the model still would not account for uncertainties in the process conditions and in the inevitable modeling errors and thus utilizing the model for online estimation and control purposes would be impractical. The model could, however, be applied to process control purposes in an offline manner. For instance, the model could be used to compute a process output map over a certain range of operating

parameters and this map could then be used for process optimization, as demonstrated in [24]. Other aspects related to process control are discussed further in Sect. 3.

3 Model-based microvia fill process control

3.1 The control approach

The basic model developed in Sect. 2 is highly detailed and enables studying and experimenting with a wide variety of process features. Thus, by comparing the model behaviour with data measured from carefully designed experiments, it can be a useful tool for improving the operator's understanding of the process and in designing the via fill process. However, to be useful for automatic control, the model should be robust, and give a good estimate of the process behaviour on average regardless of what the exact process operating conditions are and whether or not they are known in advance. Obtaining such a control model evidently requires simplifying the details of the model into a handful of basic phenomena and including the rest of the process features and details as uncertainties, or noise terms, that can be treated by a filter included in the control algorithm. Such a filter reduces uncertainties [25] using their statistical properties. Another and a simpler approach is to use averaging controls and to analyse the consequences of the control error due to using the simpler controls. In either case, the control algorithm—and so also the model when used as estimator—should not depend on unobserved variables, but be completely reliant on available measurements like cell current, voltage, temperature and so on. Also, for the purpose of practical realization, the number of algorithm parameters should be significantly lower than in the detailed model.

In the following section, the basic via fill model is dramatically simplified with the following assumptions:

1. Mass transfer of species in the very vicinity of the copper surface is dominated by diffusion
2. Electrochemical side reactions on the cathode are negligible and the rate of copper reduction is directly obtained through the current measurement
3. The diffusion layer can be simplified into one dimension with a varying thickness, meaning that mass transfer of copper occurring in the radial direction inside the via is negligible
4. All other phenomena affecting the via fill process can be considered as uncertainties, whose average effect on the process outcome can be predicted by filtering or other means using their statistical properties

The main goal of the microvia fill process control is to maximize production while retaining product quality, with a set of process and product parameters being given. It is anticipated, that the case-specific maximal plating rate is obtained when the copper ion concentration at the cathode surface is driven to such a level that mass transfer of the copper ions to the cathode is maximized but the surface is still not depleted of copper ions. If depletion would occur, product quality would deteriorate. Although the control problem is a maximization problem with constraints, a much simpler regulator problem is solved in practice. The control is implemented by adjusting the

cell current. As the microvias only form a fraction of the PCB surface area, the cell current essentially determines the plating rate on the flat surface of the PCB but not so much inside the via, where the surfactants alter the deposition process significantly. Hence, although the current density is high inside the via, only a small fraction of the overall cell current goes through the via. Therefore, the control signal (current density) is computed in a single, representative point on the flat PCB surface so that the copper concentration on the surface is preserved at a desired level. The computed current is then utilized to find the required voltage between the electrodes by solving the Butler–Volmer equation for voltage, with the current being given. Then, as the solved cell voltage is fed back to the Butler–Volmer equation, the current density distribution over the cathode, including inside the via, is obtained and can be used in the model for validating the control signal. In the computational model we calculate the surface overpotential instead of the cell voltage.

To summarize, with the given simplifications, the process model becomes a dynamic distributed parameters model (PDE) in one spatial dimension. Thus, the model geometry is a line, whose end points are the model boundaries. The first boundary is in the bulk solution end of the considered electrolyte layer and the other end is on the cathode surface. The effects of the via geometry curvature, mass transfer effects of other species, diffusion inside the via etc. are all considered as uncertainties of the control model. The following sections describe the control model and the uncertainties in further detail.

3.2 The control model without noises

The one-dimensional diffusion system is described in Fig. 3. As no other species but the reducing copper ion are considered, only c is used to denote the copper concentration (i.e. $c = c_{\mathrm{Cu}}$). The system is considered symmetric in all other directions but that

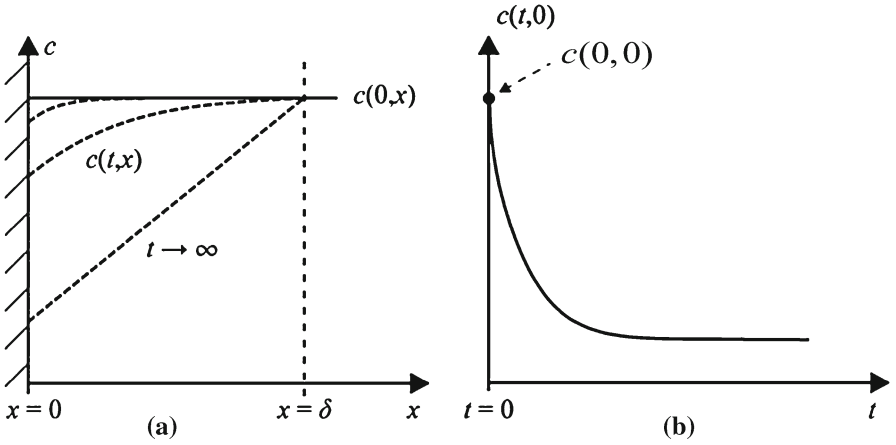

Fig. 3 Schematic 1D diffusion model illustration. The *dashed lines* in subfigure **a** illustrate the reactant concentration profile evolution after imposing a constant mass flux over the reaction surface (corresponding to a constant current on the electrode). Subfigure **b** illustrates the reactant concentration on the reaction surface in the same case

perpendicularly away from the cathode surface. The diffusion domain ($0 \leq x \leq \delta$) is finite because the bulk electrolyte is continuously agitated (i.e. kept mixed by convective fluid flow). Here δ is the thickness of the fluid diffusion layer (a.k.a. boundary layer) within which species' mass transfer is dominated by diffusion. The dashed lines in Fig. 3(a) illustrate the evolution of the copper ion concentration profile within the diffusion layer when a constant mass flux of ions is forced over or into the cathode surface (where $x = 0$) by e.g. a constant cathodic current through the electroplating cell. Figure 3(b) illustrates the evolution of the copper ion concentration $c(t, x)$ on the reaction surface in the same case.

The copper deposition reaction takes place on the solid cathode surface and mass transfer of copper ions in the domain ($0 \leq x \leq \delta, t > 0$) is dominated by diffusion. Hence, the copper ion concentration c is given by the diffusion equation.

$$c_t(t, x) = Dc_{xx}(t, x) \tag{22}$$

Here D is the copper ion diffusivity. The initial condition is that the copper ion concentration is initially everywhere on the bulk level, i.e. $c(0, x) = c_b$. Once $t > 0$, the boundary conditions are given as a Neumann condition (23)

$$Dc_x\,(t, 0) = \frac{i_c\,(t)}{z_{Cu}F} = u(t) \tag{23}$$

on the boundary $x = 0$ and as a Dirichlet condition $c(t, \delta) = c_b$ on the other boundary. In (23), $u(t)$ denotes our control variable that is directly related to the manipulated variable: the cell current. Coincidentally, u is also the mass flux (mol/m^2/s) of the plated copper. In practical systems $u(t)$ is manipulated by adjusting a voltage over the electrochemical cell in question in such a way that the total cell current corresponds to the desired control. A galvanostatic controller can be applied to set the cell current $I(t) = z_{Cu}Fu(t)/A$ on the desired level with sufficient speed.

3.3 The model uncertainties as source noises

The via fill process uncertainties can be introduced to the model as source noises. A noise term is the simplest way to simulate an uncertainty in control applications. Six categories of boundary and domain uncertainties, and respective noises, are considered:

1. Electrolyte boundary noise
2. Cathode surface boundary noise
3. Domain noise near the electrolyte boundary
4. Domain noise near the cathode surface
5. Diffusivity noise
6. Sensor noise

1. Uncertainty on the electrolyte boundary, accounted for by the noise term $\sigma_0^\delta \dot{W}_0^\delta(t)$, arises due to the uncertain thickness of the diffusion layer caused by the turbulent mixing used to keep the electrolyte as homogenous as possible. The variable

thickness of the diffusion layer is rarely known and can be estimated not better than a random variable with certain average value.

2. Uncertainties on the cathode surface (noise $\sigma_0^0 \dot{W}_0^0(t)$) arise due to unmodelled side reactions, the unmodelled two-step features of the copper reduction reaction and the inaccuracy of the control signal of a galvanostatic controller. In reality, the applied total cell current is imposed over an inhomogeneous surface with curved features, whereas the control signal was originally calculated with a 1D model which ignores surface features completely.
3. Uncertainty of mass transfer within the electrolyte close to the electrolyte boundary (noise $\sigma_j^\delta \dot{W}_j^\delta(t)$) arises due to the turbulent electrolyte flow and the related inhomogeneous convective mass transfer of species into the assumed diffusion layer. This uncertainty affects the model further inside the modeling domain than just on the electrolyte boundary. This noise is applied pointwise $j = 1, 2, 3 \ldots$ in depth of the diffusion layer.
4. Uncertainties related to the mass transfer close to the cathode surface (noise $\sigma_j^0 \dot{W}_j^0(t)$) arises due to such unmodelled phenomena like parasitic water decomposition, which agitate the electrolyte within the assumed diffusion layer and thus affect copper mass transfer there.
5. Uncertainty related to the rate of diffusive mass transfer (noise $\sigma_j^d \dot{W}_j^d(t)$) arises due to using the simplest possible diffusion model. The diffusion Eq. (22) is originally developed for dilute, non-ionic solutions while the via fill electrolyte certainly is very concentrated and includes ions. Furthermore, a constant diffusion coefficient is used while it is known that the copper ion diffusivity is nonlinearly related to its concentration and solution temperature. These simplifications create uncertainty in the entire modeling domain. Similarly, also the migration process which is omitted from the mass transfer model (22) could be considered as a mass transfer uncertainty extending over the whole domain.
6. Uncertainty related to sensor accuracy (noise $r\dot{V}(t)$) has an effect on the deposition process only if a stochastic feedback control is applied, which is not the case in this paper. Instead, a feed-forward control which is based on an averaging model is applied and this eliminates the effects of sensor noises on the system.

To summarize, the uncertainties are incorporated in the control model by introducing the various noise terms. A noise can be either a finite dimensional white noise or an infinite dimensional (functional space) coloured noise. Using white noise corresponds to accounting for a random modeling error and using a coloured noise corresponds to accounting for systematic model error. In many cases, for example when a model is biased, the latter is of more interest. Both cases are discussed below.

3.4 The control model with finite dimensional white noise

Considering that the dominating basic characteristics of the process are described by the model given in Sect. 3.2, and that the uncertainties described in Sect. 3.3 are present in the system, then the concentration of the copper ion in the modeling domain can be modeled with the stochastic diffusion equation with a finite dimensional Wiener process (noise) included

$$dc(t,x) = Ac(t,x)dt + \sigma(x)dW(t). \tag{24}$$

Here A is the linear operator $Ac = Dc_{xx}$ or more generally operator described by $Ac = Dc_{xx} + k_0 c_x + k_r c$ with the diffusion, convection and reaction terms included; this operator generates a strongly continuous semigroup, satisfying the coercivity assumption and other standard assumptions with $D > 0, k_0 \leq 0, k_r \leq 0$, as is natural for an electrodeposition process. $\sigma(x)dW(t)$ is a process noise with variance σ. The fact that the Wiener process (noise) is finite dimensional means the noise is applied pointwise in the diffusion layer as a random step-function. The system noise is readily discretized and as such can be easily implemented computationally.

The initial conditions for this system are the same as for the basic system (Sect. 3.2), i.e. $c(0,x) = c_b$. However, the boundary conditions are modified in order to incorporate the uncertainties. On the cathode boundary ($x = 0$) there is a stochastic Neumann condition

$$Dc_x(t,0) + k_0 c = u(t) + \sigma_0^0 \dot{W}_0^0(t) \tag{25}$$

and on the electrolyte boundary ($x = \delta$) there is a stochastic Dirichlet condition

$$c(t,\delta) = c_{bulk} + \sigma_0^\delta \dot{W}_0^\delta(t) \tag{26}$$

By these means the uncertainties at both boundaries are introduced in the model by completing the boundary conditions with generalized white noises $\dot{W}_0^0(t)$, $\dot{W}_0^\delta(t)$ with given intensities $\sigma_0^0, \sigma_0^\delta$. In (25), $u(t)$ is the control signal yet to be defined.

From a system point of view, the concentration of species is known only on the outer boundary $x = \delta$ of the diffusion layer, where $c(t,\delta) = c_{bulk}$—elsewhere it is not observed, including on the controlled boundary $c(t, 0)$, i.e. at the electrode surface. The current related to the consumption reaction can be measured, but this yields only the mass flux over the boundary and does not indicate the concentration level there.

Furthermore, in practice we only measure a current that is corrupted with unmodelled side reactions accounted for here with a white noise $\sigma_0^0 \dot{W}_0^0(t)$ but also corrupted with a sensor noise. The sensor noise $r\dot{V}(t)$ is a generalized white noise with intensity r.

$$D\dot{\xi}(t) = u(t) + \sigma_0^0 \dot{W}_0^0(t) + r\dot{V}(t). \tag{27}$$

All of the considered white noise terms on the boundaries $\sigma_0^0 \dot{W}_0^0(t)$, $\sigma_0^\delta \dot{W}_0^\delta(t)$ and $r\dot{V}(t)$ gain their exact meaning as Ito's integrals (e.g. [26]) after being written in differential form ($\sigma_0^0 dW_0^0(t)$, $\sigma_0^\delta dW_0^\delta(t)$ and $rdV(t)$) and integrated over time.

The domain noise. Due to the structure of the deposition process uncertainties the domain noise $\sigma(x)dW(t)$ can be decomposed by intensities in the boundary-related $\sigma^0(x)$, $\sigma^\delta(x)$ and domain-related $\sigma^d(x)$ components as follows

$$\sigma(x) = \sqrt{\left(\sigma^0(x)\right)^2 + \left(\sigma^\delta(x)\right)^2 + \left(\sigma^d(x)\right)^2}. \tag{28}$$

The domain noise is finite dimensional expressed as a weighted sum of single dimensional Wiener processes in (29). In other words, the noise is distributed spatially over the coordinate x. In reality, x is continuous but in the finite dimensional treatment, the

domain is discretised and the noise is applied in the discrete points x_j; between the points the noise stays unchanged. The domain noise can therefore be described as a sum over the points

$$\sigma(x)dW(t) = \sum_{j=1}^{N} \chi_j \sigma(x_j) dW_j(t). \tag{29}$$

In (29), the noise $W_j(t)$ is applied point-wise in each point (x_j, where $j = 1, \ldots, N$) of the interval $(0, \delta)$. $W_j(t)$ is standard Wiener process and $\sigma(x_j)$ is the noise intensity, in practice a weight function that sets the standard deviation of noise in the interval $(x_{j-1}, x_j]$. The interval intensity is approximated with the unit step function $\sigma_i = \sigma(x_j) 1_{(x_{j-1}, x_j]}(x)$ that uses the weight coefficients $\sigma(x_j)$ and indicator functions $\chi_j = 1_{(x_{j-1}, x_j]}(x)$. Similarly to the domain noises, the weights σ_j are decomposed in three components, each of them selected proportional to the coefficient ρ^κ and Gaussian kernel as given in (30). For brevity, the notation $\kappa = 0, \delta$ or d is introduced.

$$\sigma^\kappa(x_j) = \rho^\kappa \frac{2}{s^\kappa \sqrt{2\pi}} e^{-\frac{1}{2}\left(\frac{x_j - m^\kappa}{s^\kappa}\right)^2} \tag{30}$$

Here the coefficient ρ^κ scales the overall weight of noises by their type and s^κ concentrates the weight function $\sigma(x)$ to the either boundary 0 or δ. $m^\kappa = 0$ if $\kappa = 0$ and $m^\kappa = \delta$ otherwise. (The effect of function $\sigma(x)$ is demonstrated later on in Fig. 4.)

With the system of Eqs. (24)–(30), the model with uncertainties introduced as finite-dimensional white noise terms is complete. It can be utilized to generate the control signal as is shown in Sect. 4.

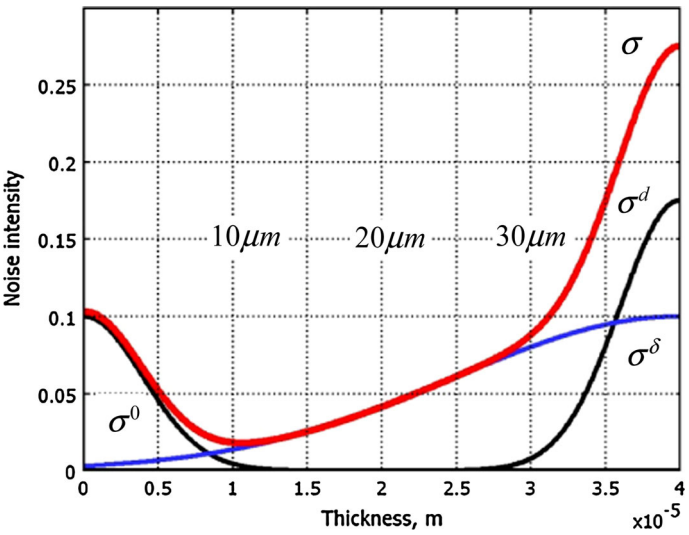

Fig. 4 The intensity of noises represents uncertainty of the applied model near the boundaries σ^0, σ^δ, within the domain σ^d, and in total σ

A detailed description of the process noises and their reasoning along with the stochastic model is given in [25]. Also the stochastic control that uses a conditionally Gaussian filter is given there. Such a feedback control can be considered reasonable as it incorporates the measurements model (27) accounting for the most relevant measurement process uncertainty effects.

3.5 The control model with coloured noise

The stochastic diffusion process model allows also for the description of the systematic model errors by completing it with colored noise, instead of white noise. In terms of the simplest derivation, the model must be completed with a functional space noise, more specifically, with an infinite dimensional cylindrical Wiener process as follows:

$$dc(t,x) = Ac(t,x)dt + \sum_{\kappa=0,\delta,d} \sigma^{\kappa}(x)\sqrt{B^{\kappa}}dW^{\kappa}(t,x). \tag{31}$$

Here B^{κ} is a linear operator that can be a trace class operator (for coloured noise) or the identity operator $B^{\kappa} = I$ (for white noise). $W^{\kappa}(t,x)$ is a cylindrical Wiener process that depends on the spatial coordinate x as a Brownian sheet which allows simple factorisation of the spatial and time dependent variables as expressed in (32)

$$W^{\kappa}(t,x) = \sum_{n=1}^{\infty} e_n^{\kappa}(x)W_n^{\kappa}(t). \tag{32}$$

Here $(e_n^{\kappa}(x) : n = 1,2,\ldots)$ is a complete orthonormal set of eigenfunctions and $(W_n^{\kappa}(t) : n = 1,2,\ldots)$ is a sequence of mutually independent Brownian motion (standard Wiener process) on a canonical probability space.

The Laplace operators A and B^{κ} with mixed boundary conditions have complete orthonormal sets of eigenfunctions. The eigenvalue problems are defined for four realizations of the Laplace operators as follows

$$A\phi_n(x) = -\alpha_n\phi_n(x), \quad B^{\kappa}e_n^{\kappa}(x) = \beta_n^{\kappa}e_n^{\kappa}(x). \tag{33}$$

Here $Ac = D\Delta c$, Δ is the Laplacian that corresponds to the mixed Neumann–Dirichlet homogeneous boundary and D is the diffusion coefficient. The eigenvalues of operator A are

$$\alpha_n = Da_n^2, \quad a_n = \left(n - \frac{1}{2}\right)\frac{\pi}{\delta} \tag{34}$$

and eigenvectors are

$$\phi_n(x) = \sqrt{\frac{2}{\delta}}\cos\left(a_n x\right). \tag{35}$$

Similarly, $B^{\kappa}c = D\Delta c$, where Δ is the Laplacian that corresponds to the mixed Neumann–Dirichlet homogenous boundary if $\kappa = 0$. If $\kappa = \delta$ or d, then Δ

corresponds to the Dirichlet–Neumann homogenous boundary. The eigenvalues of the operators B^{κ} are

$$\beta_n^{\gamma} = \frac{D}{a_n^{\gamma}} \tag{36}$$

and the corresponding eigenvectors are

$$e_n^0(x) = \phi_n(x), \quad e_n^{\delta}(x) = e_n^d(x) = \sqrt{\frac{2}{\delta}} \sin(a_n x), \tag{37}$$

In Eq. (36), γ is the noise correlation exponent that characterizes strength of noise correlation spatially. If $\gamma = 0$, we have a white noise and, if $\gamma > 0$, this is a colour noise.

A detailed description of the stochastic model with functional space noises is given in [27] and therefore further details of the model are omitted from this text.

3.6 The reference system

In the case of a linear equation, the mathematical expectation of the evolution process $m(t, x) = \mathbf{M}c(t, x)$ coincides with the noise-free process that satisfies a system similar to (38) and (39),

$$dm(t, x) = Am(t, x)\, dt, m(0, x) = c_0(x), \tag{38}$$

$$Dm_x(t, 0) = u(t), m(t, \delta) = c_{bulk}. \tag{39}$$

This is recalled below as the noise-free deterministic system or as the *reference system* for short. Note that technically the reference system (38) and (39) is identical to the original, physics-based process model (22) and (23) although they represent two conceptually different views to the same phenomenon. It can be considered that the physical system has already averaged out all possible stochastic effects and considers the natural phenomenon as exactly the average process, whereas the reference system attempts to maintain the idea of stochastic effects included.

3.7 The system control

The control target. The aim of the control is to bring the (unobserved) boundary concentration $c(t, 0)$ of copper ions at the cathode surface to level c_d which is as low as possible to maximize mass transfer of copper to the cathode without depleting, and thus deteriorating, the surface completely. The target is set as a fixed concentration level c_d, and not as a time-dependent function, which simplifies the control problem essentially: instead of a tracking problem it is a regulating problem. In the case of via fill process, the depletion in the via is avoided by selection of the corresponding target c_d on the flat surface level.

Although tracking controls can be found for the finite and semi-finite diffusion processes, they are relatively complex. Furthermore, the controls are further compli-

cated if they are generalized for a partially observed diffusion process [28] or generalized for a stochastic process such as (24)–(30) or (31)–(37). For practical purposes, however, a regulating boundary control is assumed sufficient.

The boundary control. The proportional control law

$$u(t) = -K_P\,(m(t,0) - c_d) \tag{40}$$

brings the concentration of the averaged system (38) and (39) or the concentration of the noise-free system (22) and (23) close to the desired level c_d. The bigger the control gain K_P is, the closer and faster the controlled concentration comes to the desired level c_d. However, such a proportional control always leaves a static control error c_d^0.

$$c(t,0) - c_d \to \frac{D}{D + K_P\delta}\,(c_{bulk} - c_d) \equiv c_d^0. \tag{41}$$

The static control error can be removed entirely if the target concentration is selected appropriately, specifically, if $c_d - c_d^0$ is used as target. The control (40) is then an exponentially stabilizing. This feed-back boundary control (40) can be expressed [29] as the feed-forward control (42) that does not require concentration measurements on the boundary.

$$u\,(t) = -K_P\,(c_{bulk} - c_d)\left(\frac{D}{D + K_P\delta} + 2K_P D\sum_{n=1}^{\infty}\frac{e^{-\mu_n^2 Dt}}{\delta K_P^2 + K_P D + \mu_n^2\delta D^2}\right) \tag{42}$$

In Eq. (42), μ_n are the roots of the transcendental Eq. (43):

$$\frac{D}{K_P}\mu + \tan\,(\mu\delta) = 0 \tag{43}$$

These roots can be found fast. (Convergence to three-digit accuracy occurs in ca. 10 steps.) The sequence of roots increases so rapidly $\mu_n \to \infty, n = 1, 2, \ldots$ that the sum (42) converges in ca. 50 steps.

The control effort (40) is initially at its maximum value, $u(0) = -K_P(c_{bulk} - c_d)$. If necessary, the control effort can be decreased with a time-variable gain, $K_P(t) = K_P(1 - e^{-\nu t})$, $\nu \geq s0$.

The same control law in either modification (40) or (42) can be applied for control of the stochastic system and if we do so, a control error, in this case better called a residual, (44) emerges.

$$\varepsilon(t,x) = c(t,x) - m(t,x) \tag{44}$$

This residual is induced by the stochastic noise and application of the deterministic controls (40) or (42) instead of a stochastic control (e.g. [25]). The control error is almost irreducible in the presence of white noise but reducible to a wide extent in the case of coloured noise (i.e. systematic model errors). The probabilistic properties of

the residuals have been found in the cases of finite dimensional noise [29] and infinite dimensional noise [27], along with the propagation of the uncertainties in space-time. It is found, as shown below, that even a relatively weak correlation of colored noises improves the model and control quality significantly.

4 Evolution of system noises and process control: numerical results

At first we demonstrate the effect of noises (uncertainties) on the controlled process in simple cases and then we apply the discussed controls on the detailed microvia filling process model.

4.1 Case I: control model with white noise

The parameters that are used in the simulation are summarized in Table 2. The physical parameters have similar values as in Sect. 2 and as found in [23]. The noise parameters were chosen more formally as shown in Fig. 4.

The unobserved concentrations generated by stochastic model (24)–(26) in the presence of feedback control (40) are shown in Fig. 5 along with estimated concentrations from (38) to (39). Despite the incomplete measurements and relatively high noise level, the estimated process follows the true concentration quite closely. The mean value curves are rather smooth in Fig. 5 due to the set constant $m(t,\delta) = c_{bulk}$ on one boundary and stabilization of the process at constant target $m(t,0) = c_d$ on the other boundary. Higher regularity inside the domain and lower regularity on the boundary is the standard features that a Laplacian conveys.

Table 2 Electrodeposition process parameters

	Coefficient	Value	Unit
Electrolyte properties	c_{bulk}	780	mol/m^3
	D	4×10^{-10}	m^2/s
Domain noise focus	s^0	4×10^{-6}	m
	s^δ	4×10^{-6}	m
	s^d	1.5×10^{-5}	m
Domain noise intensity	ρ^0	0.1	mol/m^3
	ρ^δ	0.175	mol/m^3
	ρ^d	0.1	mol/m^3
Boundary noise intensity	σ_0^0	1×10^{-4}	mol/m^2
	σ_0^δ	1.2	mol/m^2
Noise spatial correlation power	γ	0	–
Control target, gain and discount factor	c_d	100	mol/m^3
	K_P	1×10^{-3}	m/s
	ν	0.2	1/s
Geometry	δ	4×10^{-5}	m

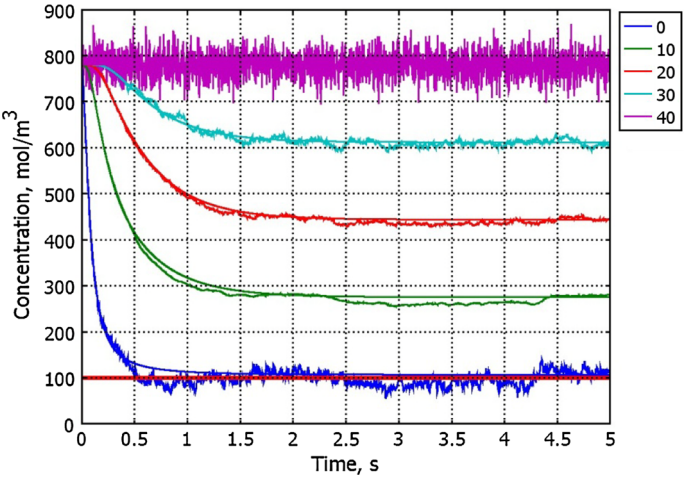

Fig. 5 The simulated (noisy) and estimated (smooth) concentration of copper(II) within the diffusion layer at distances $x = 0, 10, 20, 30, 40\,\mu$m. The simulated concentration at the cathode surface and its estimated value are close to the target concentration of 100 mol/m^3 (*solid horizontal red line*)

Table 3 Electrodeposition process parameters in Case II

	Coefficient	Value	Unit
Domain noise focus	s^0	4×10^{-6}	m
	s^δ	4×10^{-6}	m
	s^d	8×10^{-6}	m
Domain noise intensity	ρ^0	3.5×10^{-4}	mol/m^3
	ρ^δ	3.5×10^{-4}	mol/m^3
	ρ^d	1×10^{-4}	mol/m^3
Boundary noise intensity	σ_0^0	1.5×10^{-4}	mol/m^2
	σ_0^δ	3.5	mol/m^2
Noise spatial correlation power	γ	0 and 0.5	–

The stabilized process at the boundary reaches almost the desired level in Fig. 5. A small static error is visible. This error is almost insignificant and can be removed entirely as was discussed above.

4.2 Case II: control model with coloured noise

In this section some of the noise parameters are increased significantly on purpose to demonstrate the robustness of the control. The simulation parameters are given in Table 3.

At first we consider the white noise case, when the noise correlation exponent is set at zero, $\gamma = 0$. Figure 6 shows the control error (residual) obtained from a large number (2,500) of realizations of the stochastic system when simulating the copper concentration in the diffusion layer. The control error is distributed over a wide region

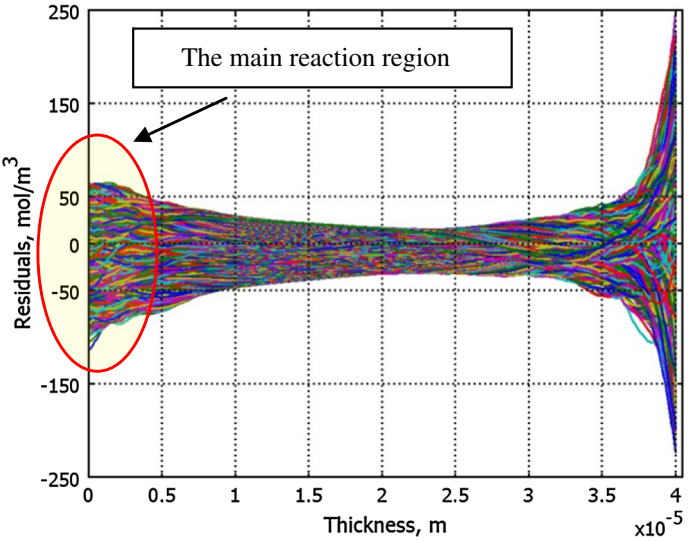

Fig. 6 The effect of source noises on control errors (residuals) is spread over the diffusion layer. In this worst-case scenario, the model with white noise is significantly uncertain in the region of main reaction

from the cathode to the bulk end. The closest region to the cathode is the crucial part of the electrodeposition reaction and the current model is very uncertain there. As the stochastic system (Eqs. (31)–(37)) is controlled based on the averaged system (Eqs. (38), (39)), the copper concentration can in this case reach a depletion level, i.e. zero concentration (which occurs if the residual $\varepsilon(t, 0) \leq -100$ in Fig. 6) due to the existing uncertainties.

The coloured noise case is considered next, with moderate noise correlation $\gamma = 1/2$. As result of noise spatial correlation, the residuals are clearly suppressed.

Figure 7, compared to the case without noise correlation, Fig. 6. The control model is more certain in the most important region for the electrodeposition reaction, at the cathode. Hence a systematic model error has been removed efficiently.

The chosen colour noise improves the control situation radically, so much so that there is no need for more intensive smoothing with colour ($\gamma > 1/2$). On the contrary, it is possible to use less correlation [27]. For example, $\gamma = 1/8$ provided about 40 % less variation than the white noise did. Eventually, however, the control errors are lower bounded by the effect of boundary noises, which cannot be reduced unless they are temporarily correlated. (This case is not presented.)

These simulations above demonstrate that the source noises expand with attenuation in space-time. Even though a relatively simple boundary control (40) or (42) is applied the control errors are bounded everywhere in the diffusion layer and are limited on the boundaries [27,29]. The control law applied here and all of its derivatives are smooth functions [29]. Generally boundary controls of distributed parameter systems are not so well behaving and are rough functions [30].

Many more details of propagation of the source noises in space-time are given in [27,29] in both white noise and colored noise cases. Understanding the propagation

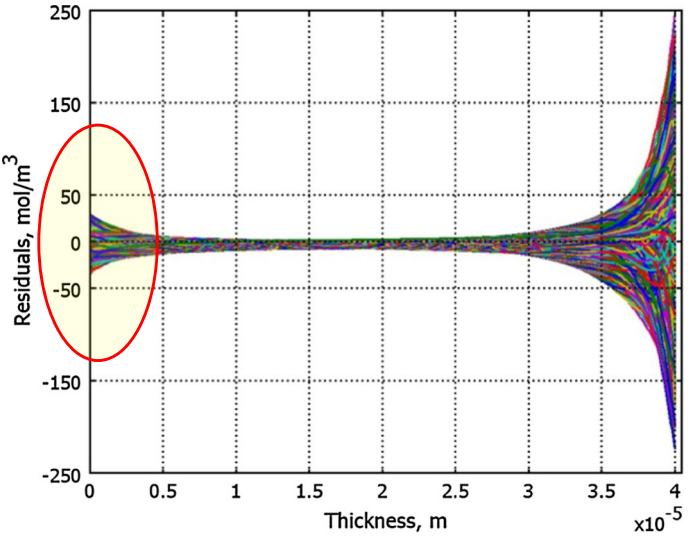

Fig. 7 The effect of source noises is suppressed effectively. The remaining effect is mostly that of the boundary noises while the effect of domain noise is diminished. (It is smoothed out by the presence of correlation of the noises.) The model with coloured noise is less uncertain in the region of the main reaction. *Note* also that the same source noise intensity is applied here as in the simulations for Fig. 6

properties help to interpret the measured process data and to distinguish the physical phenomena from the effects induced by the uncertainty in the applied model.

4.3 Case III: control application to the viafill process

In case III, Eq. (40) is used to calculate the control signal for the microvia fill process modeled with the detailed process model, developed in Sect. 2. It is considered that the detailed model also includes modeling errors and deviates from the "real-world process". The control algorithm then acknowledges these differences and applies an averaged control signal that in fact corresponds to the noise-free detailed model. The setpoint concentration $c_d = 600\,\mathrm{mol/m^3}$ on a single point on the flat surface was applied for calculation of the controls (40).

As said, the current computed at a single point on the flat cathode surface, is used to find the voltage required between the cell electrodes by solving a location-specific Butler–Volmer equation for voltage at a representative point, with the current being given. Then, as the solved cell voltage is fed back to the Butler–Volmer equation over the whole cathode, the current density distribution over the cathode, including inside the via, is obtained. The current density distribution induces a Cu(II) concentration field through the mass transfer system and this field on the cathode boundary is input to the control (40). This closes the control loop.

The shape of via and field of Cu(II) concentration during model-based control is shown in Fig. 8 with snapshots corresponding to four time instances. It is seen that the outcome of via shape is nearly identical to that displayed in Fig. 2. However,

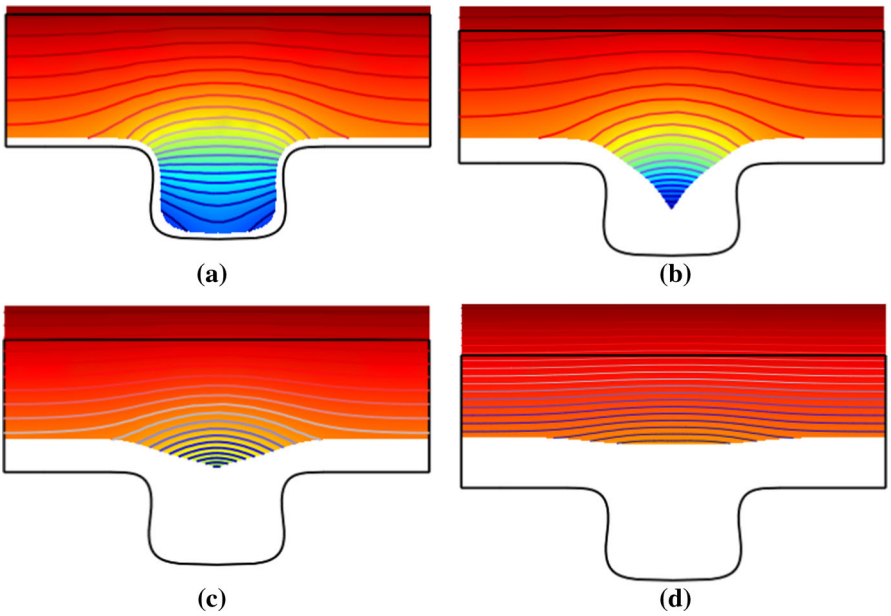

Fig. 8 Evolution of the shape of via and the Cu(II) concentration field in model-based controlled via fill process. The time instants are **a** 12, **b** 36, **c** 48 and **d** 72 min

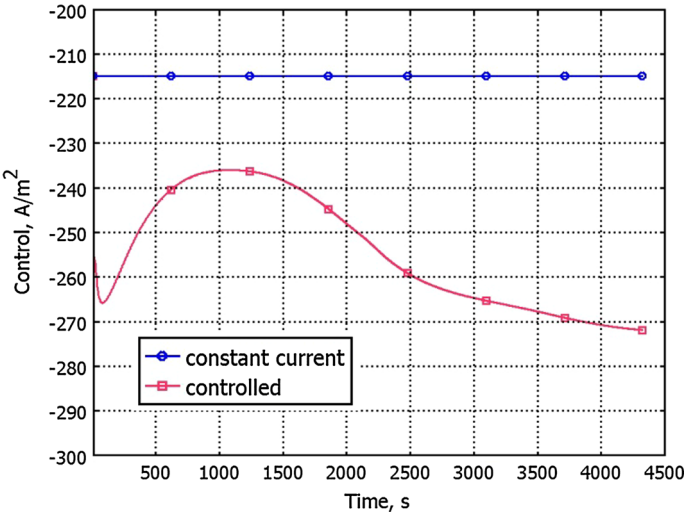

Fig. 9 The constant current and the time-varying controlled current applied to the viafill process

meanwhile Fig. 1 and 2 describe the process evolution with a constant current of 215 A posed over the cell, in the controlled case the cell current fluctuates as illustrated in Fig. 9. At first, the current changes rapidly but soon it gradually approaches a constant value. On average the controlled current is slightly higher (240–270 A) than in the constant current case. As result, the deposition process reaches the 80 % fill ratio level

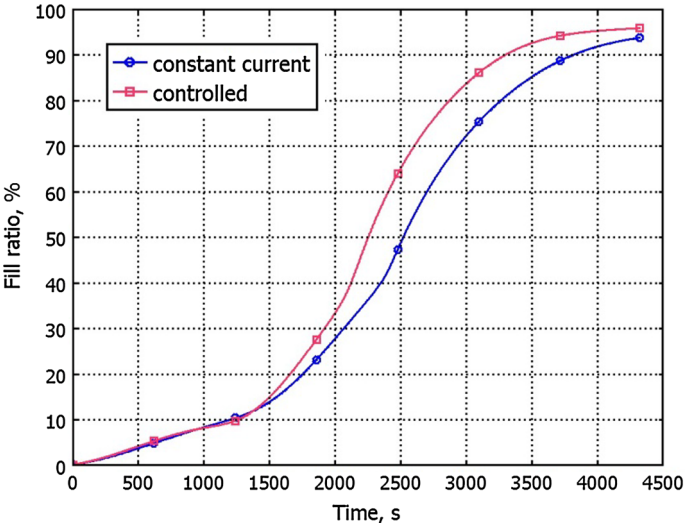

Fig. 10 The via fill ratio during the fill process when both constant and time-varying controlled plating current is used

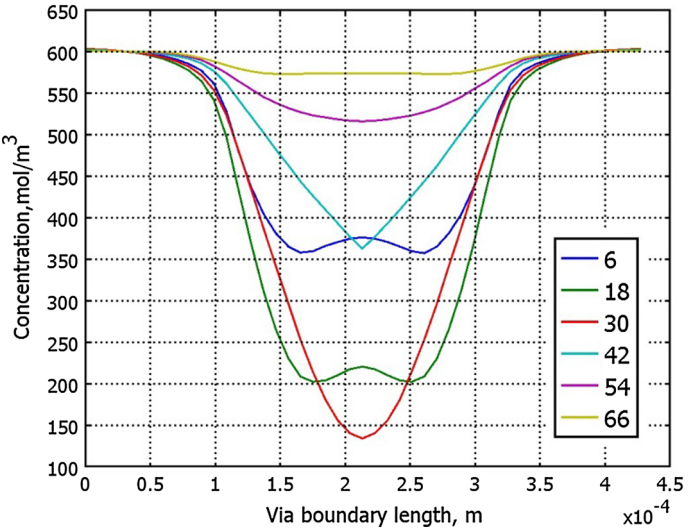

Fig. 11 The copper(II) ion concentration inside the via and at the board surface during the controlled viafill process. The electrode is not depleted as the concentration inside the via is above 100 mol/m^3 throughout the whole process. The time instants are 6, 18, 30, 42, 54 and 66 min

ca. 10 min sooner than with a constant current. The via fill ratios for both processes are shown in Fig. 10. Despite posing a larger current through the cell, the control is safe because the concentration in via never went below 100 mol/m^3, illustrated in Fig. 11. The obtained control indicates that in this case, we can run the viafill process safely if we insure that the copper ion concentration at the flat cathode surface stays above 80 %

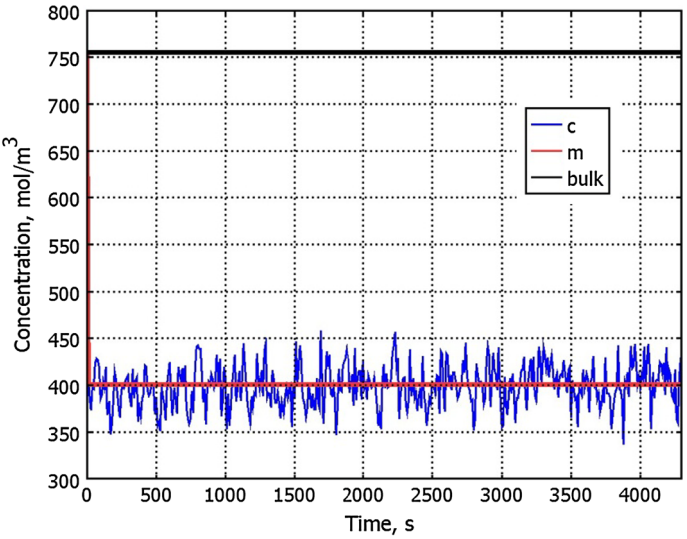

Fig. 12 The copper(II) ion concentration at the board surface during the controlled viafill process with uncertainties (c) and without uncertainties (m)

of the bulk concentration value. The main benefit of the control algorithm, however, is that it automatically offers the optimal means to carry out the plating process in whichever case comes to question when the detailed model and parameters are given.

The control errors induced by via fill uncertainties can be analyzed in the same manner as demonstrate in Subsects. 4.1 and 4.2. However, in the stochastic model case the target should be chosen lower $c_d = 400\,\mathrm{mol/m^3}$ than in the detailed model case that compensates for the ignored processes. The controlled stochastic process $c(t, 0)$ fluctuates around the target (Fig. 12) while the averaged process $m(t, 0)$ is maintained exactly on the target. The fluctuation from target is less in the case of stochastic field (2D model) and smallest in the case of coloured noise. The 2D via fill model with finite dimensional noise does not raise regularity problems but the model with functional space noise is more irregular and only a coloured noise can be applied in the 2D via fill case [31,32].

5 Conclusions

An overview of the modeling and model-based control of the microvia fill process was given. A basic configuration for a distributed parameters model of the microvia fill process was given first. The model appropriateness was illustrated by comparing model output with measured data. This model is highly detailed and informative, and therefore enables studying and designing the process in an illustrative, quantitative manner. Such a process model is, however, often too complex and too sensitive to e.g. errors in model parameters to be used for automatic process control purposes. Hence, a simpler and more robust stochastic process model was given to work around these problems was also given. The stochastic model was utilized for model-based process

control development and the control algorithm simulations were used to illustrate the control effectiveness. Finally the developed control was applied to control the detailed microvia fill process model.

Acknowledgments Timo Närhi of Meadville Aspocomp Intl. Ltd. is thanked for his comments on PCB manufacturing today.

References

1. T.P. Moffat, D. Wheeler, W.H. Huber, D. Josell, Electrochem. Solid-State Lett. **4**, C26–C29 (2001)
2. T.P. Moffat, D. Wheeler, D. Josell, Electrochem. Soc. Interface **13**, 46–52 (2004)
3. T.P. Moffat, D. Wheeler, S.K. Kim, D. Josell, J. Electrochem. Soc. **153**, C127–C132 (2006)
4. D. Josell, T.P. Moffat, D. Wheeler, J. Electrochem. Soc. **154**, D208–D214 (2007)
5. D. Wheeler, D. Josell, T.P. Moffat, J. Electrochem. Soc. **150**, C302–C310 (2003)
6. W.-P. Dow, H.-S. Huang, Z. Lin, Electrochem. Solid-State Lett. **6**, C134–C136 (2003)
7. W.-P. Dow, H.-S. Huang, J. Electrochem. Soc. **152**, C67–C88 (2005)
8. W.-P. Dow, M.-Y. Yen, S.-Z. Liao, Y.-D. Chiu, H.-S. Huang, Electrochim. Acta **53**, 8228–8237 (2008)
9. P.C. Andricacos, C. Uzoh, J.O. Dukovic, J. Horkans, H. Deligianni, IBM J. Res. Dev. **42**, 567–574 (1998)
10. P.M. Vereecken, R.A. Binstead, H. Deligiani, P.C. Andricacos, IBM J. Res. Dev. **49**, 3–18 (2005)
11. A.C. West, J. Electrochem. Soc. **147**, 227–232 (2000)
12. A.C. West, S. Mayer, J. Reid, Electrochem. Solid-State Lett. **4**, C50–C53 (2001)
13. Y. Cao, P. Taephaisitphongse, R. Chalupa, A.C. West, J. Electrochem. Soc. **148**, C466–C472 (2001)
14. M. Lefebvre, G. Allardyce, M. Seita, H. Tsuchida, M. Kusaka, S. Hayashi, Circuit World **29**, 9–14 (2003)
15. J.F. Coombs Jr, *Printed Circuits Handbook (eBook)*, 6th edn. (McGraw-Hill, New York, 2008)
16. J. Donea, A. Huerta, *Finite Element Methods for Flow Problems* (Wiley, New York, 2003)
17. A. Pohjoranta, R. Tenno, J. Electrochem. Soc. **154**, D502–D509 (2007)
18. T.P. Moffat, D. Wheeler, S.K. Kim, D. Josell, Electrochim. Acta **53**, 145–154 (2007)
19. Y. Kaneko, Y. Hiwatari, K. Ohara, Mol. Simul. **30**, 895–899 (2004)
20. T.J. Pricer, M.J. Kushner, R.C. Alkire, J. Electrochem. Soc. **149**, C406–C412 (2002)
21. X. Li, T.O. Drews, E. Rusli, F. Xue, Y. He, R. Braatz, R. Alkire, J. Electrochem. Soc. **154**, D230–D240 (2007)
22. A. Pohjoranta, R. Tenno, Eng. Comput. **27**, 165–175 (2011)
23. R. Tenno, A. Pohjoranta, J. Electrochem. Soc. **155**, D383–D388 (2008)
24. R. Tenno, A. Pohjoranta, Int. J. Control **82**, 883–893 (2009)
25. R. Tenno, Int. J. Control **85**, 1807–1826 (2012)
26. I. Karatzas, S. Shreve, *Brownian Motion and Stochastic Calculus*, 2nd edn. (Springer, Berlin, 1991)
27. R. Tenno, Evolution of the regulation errors in the diffusion layer in electrodeposition process control. IFAC J. Proc. Control **24** (2014, in press)
28. R. Tenno, A. Pohjoranta, Simul. study IFAC J. Proc. Control **22**, 228–235 (2012)
29. R. Tenno, IFAC J. Proc. Control **24**, 82–92 (2014)
30. J.L. Lions, *Optimal Control of Systems Covered by Partial Differential Equations* (Springer, Berlin, 1971)
31. G. Da Prato, J. Zabczyk, *Stochastic Equations in Infinite Dimensions* (Cambridge University Press, Cambridge, 1992)
32. G. Da Prato, *Kolmogorov Equation for Stochastic PDEs* (Springer, Berlin, 2004)